Journal of the European Ceramic Society 22 (2002) 559–566

www.elsevier.com/locate/jeurceramsoc

Elevated temperature strength and thermal shock behavior of hot-pressed carbon fiber reinforced TiC composites

Gui-Ming Song[a,*], Ying Wu[b], Qiang Li[a,c]

[a]*School of Materials Science and Engineering, PO Box 433, Harbin Institute of Technology, Harbin 150001, PR China*
[b]*Beijing General Research Institute of Mining and Metallurgy, Beijing 100044, PR China*
[c]*School of Materials Science and Engineering, Fuzhou University, Fuzhou 350002, PR China*

Received 11 January 2001; received in revised form 11 April 2001; accepted 28 April 2001

Abstract

In order to improve the elevated strength and thermal shock resistance of TiC materials, 20vol% short carbon fiber-reinforced TiC composite (C_f/TiC) was produced by hot pressing. With carbon fiber addition, the strength and fracture toughness of TiC is increased remarkably, and the elastic modulus and thermal expansion coefficient are decreased. The strength value of C_f/TiC composite is 593 MPa at room temperature and 439 MPa at 1400°C, and the fracture toughness value at room temperature is 6.87 MPa $m^{1/2}$. The thermal stress fracture resistance parameter, R, thermal stress damage resistance parameter, R^{IV}, and thermal stress crack stability parameter, R_{st}, are all increased. The residual strength decreases significantly when the thermal shock temperature difference, ΔT, is higher than 900°C, and the residual strength is 252 MPa when ΔT is 1400°C. Carbon fiber reinforced-TiC composite exhibits superior resistance to thermal shock damage compared with monolithic TiC. The catastrophic failure induced by severe thermal stresses can be prevented in C_f/TiC composite. © 2002 Elsevier Science Ltd. All rights reserved.

Keywords: Carbon fiber; Composites; Mechanical properties; Thermal shock resistance; TiC

1. Introduction

As one of the most promising high-temperature ceramic materials, TiC has been under active development for demanding elevated temperature applications for its unique combination of higher melting point (~3067°C), good strength, good thermal stability and corrosion resistance.[1,2] However, like most other kinds of ceramics it has a tendency toward catastrophic failure, especially upon severe thermal shock (a sudden change in temperature), which remains a major obstacle to its more widespread utilization. TiC can be toughened and strengthened with the addition of particles (such as SiC, TiN, WC, NbC and TiB_2)[3–5] and/or metal elements (such as Ni, Mo, Cr, Co, etc.).[1,6] Unfortunately, the toughness of TiC materials reinforced by ceramic particles needs to be further improved to withstand the thermal shock, and the relatively low melting point of the metallic binder alloys Ni–Mo, Ni–Mo–Al, Ni–Cr and Ni–Co–Cr[3] limits the application of these TiC materials reinforced by metal elements at higher temperature (such as 1400°C). Recently, it has been shown that intermetallic aluminides can be utilized as binder phase to prepare TiC composites, such as TiC–Ni_3Al[7] and TiC–FeAl.[8,9] These composites were found to have promising mechanical properties comparable to that of commercial TiC-Ni. Durlu has also reported TiC-iron silicide and TiC-iron aluminide composites possessing high hardness and good bending strength.[10] Nevertheless the high temperature strengths of these materials need to be further improved.

In order to avoid or mitigate catastrophic failure of monolithic ceramics during thermal shocking, ceramic matrix composites reinforced by fibers, whiskers and particles have been widely researched and developed.[11] Various thermal shock studies have been conducted in this field, mainly studying Al_2O_3, ZrO_2, SiC, Si_3N_4, SiO_2 and their composites.[12–14] These studies show that whiskers or short fibers or long fibers additions increased the thermal shock resistance of the composites. The research work of Kamiya et al.[15] on the TiC ceramics reinforced by 10 vol.% SiC whiskers has shown that SiC whiskers remarkably increased the fracture toughness and strength

* Corresponding author. Tel.: +86-451-6414291; fax: +86-451-6413922.
E-mail address: songguim@hotmail.com (G.-M. Song).

0955-2219/02/$ - see front matter © 2002 Elsevier Science Ltd. All rights reserved.
PII: S0955-2219(01)00308-9

of TiC, which demonstrates a bright prospect of ceramic whisker or fiber in strengthening TiC. Unfortunately, a drawback to the use of whiskers has been identified that the whisker is a potential health hazard.[16] The feasibility of carbon fibers as structural materials in aerospace and aeronautic industries has been demonstrated, considering their high strength, low density and good thermal stability, and also they are very good reinforcements in strengthening or/and toughening ceramics and improving thermal shock resistance of ceramics. For examples, carbon fiber reinforced SiC composites [17] and carbon fiber reinforced SiO_2 composites [14] exhibit good high temperature strength, toughness and high thermal shock resistance. However, to date, few studies have been carried out on TiC composites reinforced by carbon fibers.

In this study, in order to improve the elevated temperature strength and thermal shock resistance of TiC so as to extend the applications in high temperature environment, TiC composite containing 20 vol.% short carbon fibers (C_f/TiC) is prepared by hot pressing, and the effect of carbon fibers on the elevated temperature strength and thermal shock resistance of the composites is investigated.

2. Experimental procedure

The characteristics of the commercial TiC powders and short carbon fibers used as starting materials in this study is given in Table 1. TiC powders and 20 vol.% carbon fibers were mixed in ethanol for 24 h in a plastic jar before compaction. Zirconia balls 5–10 mm in diameter were used as milling balls. The resulting slurry was dried at 100°C, and then compacted by cold pressing at 200 MPa in a steel mould. The compacted samples were hot pressed in a graphite mould to discs of 55mm in diameter and 10 mm in height at 2100°C under 30 MPa for 1 h in a vacuum of 1.3×10^{-3} Pa. For comparison with the C_f/TiC composite, monolithic TiC was also produced using the same hot-pressing technique.

The flexural strength was measured by a three point bending test with a span of a 20 mm and a crosshead of 0.5 mm/min at room and high temperature. The dimension of flexural strength test bars was $30\times3\times4$ mm^3. Strength measurement was carried out in air at room temperature and in an argon atmosphere at high temperature on an Instron-type machine. To measure strength at high temperature, the samples were placed in an electric furnace and held at the required temperature for about 10 min. Temperatures were measured with Pt-Rh thermocouples placed near the samples. Fracture toughness was evaluated by a single-edge notched beam test with a span of a 16 mm and a crosshead speed of 0.05 mm/min using test bars of $2\times4\times20$ mm^3 with a notch of 2 mm in depth and 0.2 mm in width. Load–strain curves were recorded by attaching strain gauges to the tensile surfaces of specimens. All flexural bars were fabricated with the tensile surface perpendicular to the hot-pressing direction. The density was measured by the Archimedes water-immersion method.

Thermal expansion only along the direction vertical to the hot-pressing direction was measured from room temperature to 1000°C with a commercial thermomechanical analyzer. The specimen size was $3\times4\times10$ mm^3. Measurement of thermal diffusivity along the direction vertical to the hot-pressing direction was carried out using a laser-flash technique, and the specimen size was $\phi10\times(1.5–2)$ mm^3.

In order to evaluate the thermal shock resistance, a water quenching tests under argon atmosphere were conducted. Sets of five or six specimens were held at a predetermined temperature for 10 min on a SiC board which was then tilted to drop the specimens into a container of room-temperature water. The residual strengths of the shocked specimens were measured under the same conditions as those of the unshocked ones. The microstructure and the fracture characteristics of C_f/TiC composites before and after thermal shock were examined using a scanning electron microscope (SEM).

Table 1
Characteristics of carbon fiber and TiC

	Carbon fiber	TiC
Density, g/cm^3	1.76	4.93
Purity, %	>98	>98
Size	2 mm in length and 6–8 μm in diameter	Average diameter of 2.5 μm
Thermal expansion coefficient, $\times10^{-6}$ K^{-1}	−1.0 to −0.5 (fiber axial direction)	7.76 (293–1300 K)
	7–12 (fiber radial direction)	10.4 (1300–2300 K)
Elastic modulus, GPa	230	460–500
Poisson's ratio	–	0.25
Melting point, °C	3400 (sublime)	3067
Thermal conductivity, W m^{-1} K^{-1}	55.8	33.67
Strength, MPa	~2700 (tensile strength)	–
Elongation, %	~1.4	<0.5

3. Results and discussion

3.1. Microstructure

Fig. 1 is a micrograph of the polished surface of the C_f/TiC composite, revealing that the carbon fibers were uniformly distributed in the TiC matrix. Although raw carbon fibers possess a high aspect ratio, ~300 (2000 μm in length, 7 μm in diameter), and they are prone to be twisted during mixing, the wet ball-milling technique can effectively prevent fibers from aggregating. On the other hand, the length of the fibers exposed on the polished surface of the specimen is about 20–180 μm (average length is estimated as ~120 μm), which is much less than the initial length (2000 μm) of the fibers. In fact, it is also very difficult to find a longer fiber (> 500 μm) on the polished surfaces, indicating that the length of the fibers has been remarkably changed after the ball-milling and hot-pressing processes. The fiber length decreasing may be explained as follows. Firstly, fibers are damaged and then fractured due to the colliding of the milling balls, which is the main reason for the shortened fibers. Secondly, some fibers fractured due to the volume shrinkage of the green bodies during hot pressing.

The relative density of monolithic TiC is 98.2%, which is higher than that of the C_f/TiC composite (97.6%). It is difficult to get a full dense monolithic TiC at 2100°C without any sintering aid,[18] the difficulty of TiC densification is increased when carbon fiber is added due to the fiber bridging effect.[19] Therefore, the relative density of the C_f/TiC composite is lower than that of monolithic TiC.

3.2. Elevated temperature strength

Degradation of fracture strengths of monolithic TiC and the C_f/TiC composite at elevated temperature are found in Fig. 2. For monolithic TiC and the C_f/TiC composite, the room temperature flexural strengths were maintained for the most part up to 1000°C, followed by a drastic drop in strength between 1000 and 1400°C. However, a higher flexural strength than that of monolithic TiC has been measured in the C_f/TiC composite at all testing temperatures as a result of the addition of carbon fibers. Especially at 1400°C, the strength of the composite is 439 MPa, an increase of 78% over that of monolithic TiC (247 MPa). The increase in strength at 1400°C is much higher than that at room temperature (78 and 26%, respectively), which shows that the strengthening effect of carbon fiber on TiC is more prominent at elevated temperature. The brittle–ductile transition temperature of TiC is around 800°C,[20] and the strength generally decreases when the temperature is higher than 800°C,[21] the strength of the composite also decreases accordingly as temperature increases.

Fig. 3 shows the fracture surfaces of the C_f/TiC composite fractured at room temperature (Fig. 3a) and 1400°C (Fig. 3b). The two fracture surfaces (Fig. 3a and b) are similar, and the pullout length of the fibers on the two surfaces is 2–30 μm, much less than the average length of the carbon fiber exposed on the polished surface of the specimen (~120 μm, see Fig. 1), which implies that the fiber fractured and then were pulled out from the TiC matrix during the fracture process of the composite. Thereby, the higher fracture strength is undoubtedly the direct contribution of the high strength of carbon fiber to the composite.

3.3. Thermal shock resistance

The curves of the residual strength, σ_r, of monolithic TiC and the C_f/TiC composite versus water-quenching temperature difference, ΔT, are plotted in Fig. 4. σ_r of

Fig. 1. The micrograph of a polished surface of the C_f/TiC composite, showing a uniform distribution of carbon fibers.

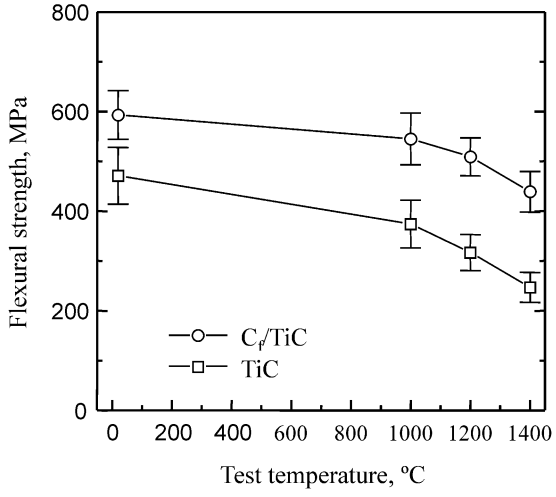

Fig. 2. Flexural strengths of the C_f/TiC composite and monolithic TiC versus testing temperatures.

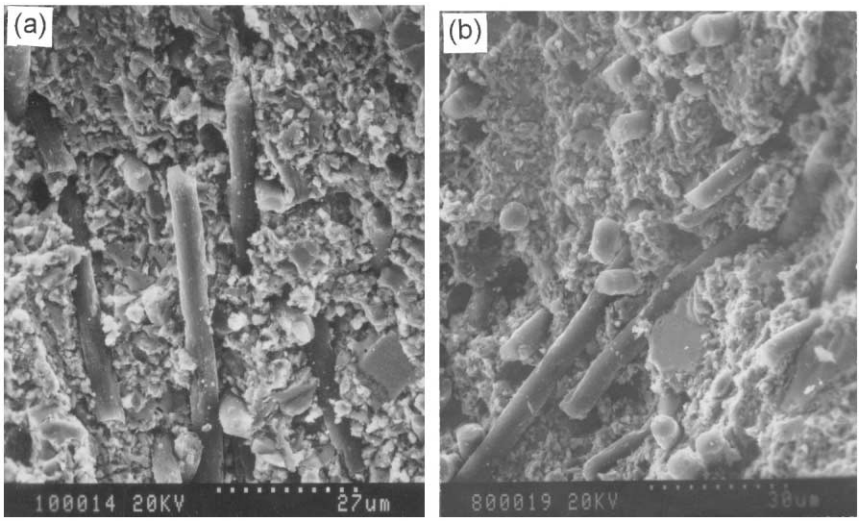

Fig. 3. Fractograph of the C_f/TiC composite fractured at room temperature (a), at 1400°C (b).

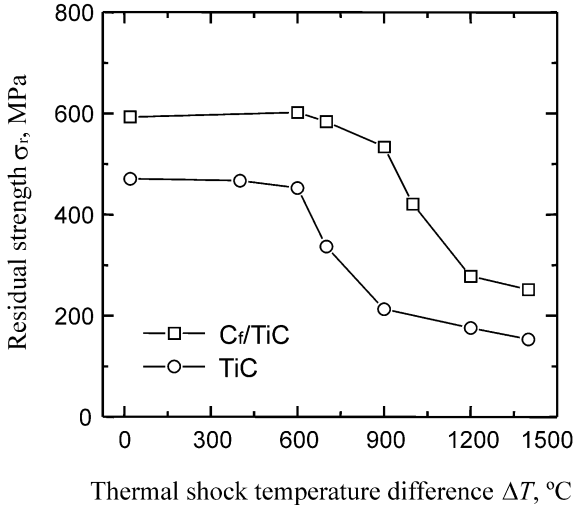

Fig. 4. Residual strength of monolithic TiC and the C_f/TiC composite thermally shocked versus thermal shock temperature differences.

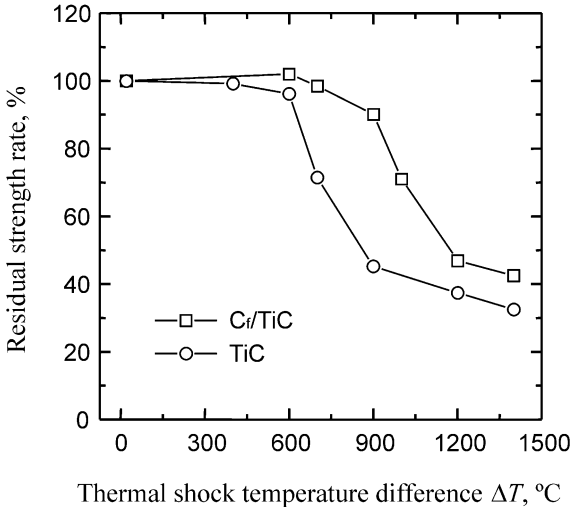

Fig. 5. Residual strength rate of monolithic TiC and the C_f/TiC composite thermally shocked versus thermal shock temperature differences.

the monolithic TiC possesses a significant portion of its original strength up to $\Delta T = 600$°C, and decreases rapidly when ΔT exceeds 600°C. For the C_f/TiC composite, σ_r maintains for the most part up to 900°C, followed by a drastic drop from 900 to 1400°C. σ_r of C_f/TiC composite is 252 MPa at $\Delta T = 1400$°C, which is higher than that of monolithic TiC (153 MPa). Fig. 5 shows the curves of the residual strength rate (the ratio of residual strength, σ_r, to original strength, σ_0) of monolithic TiC and the C_f/TiC composite, the changing trend of residual strength rate versus ΔT is similar to that of residual strength. Therefore, the addition of carbon fibers to TiC increases not only the critical temperature difference, ΔT_c, for strength degradation but also the residual strength rate from 600 to 1400°C. Consequently, the thermal shock resistance of TiC is increased by the addition of carbon fibers.

In order to further evaluate the thermal stress crack initiation and propagation behavior of C_f/TiC composites, three thermal shock resistance parameters are used: thermal stress fracture resistance parameter, R, thermal stress damage resistance parameter, R^{IV}, and thermal stress crack stability parameter, R_{st}. These parameters are usually used to evaluate the thermal shock properties of ceramics,[11, 22, 23] and they are defined, respectively, as follows:

$$R = \frac{\sigma(1-\nu)}{(\alpha E)} \tag{1}$$

$$R^{IV} = E\gamma_f/\left[\sigma^2(1-\nu)\right] \approx (K_{IC}/\sigma)^2/(1-\nu) \tag{2}$$

$$R_{st} = [\gamma_f/(\alpha^2 E)]^{1/2} \tag{3}$$

where σ is the tensile strength of the material, v is Poisson's ratio, α is the thermal expansion coefficient, E is the elastic modulus, γ_f is the fracture surface energy, and K_{IC} is the fracture toughness. R represents the critical temperature difference, ΔT_c, to which a body can be subjected without the initiation of fracture under steady state heat flow or severe transient thermal condition.[22] R^{IV} decides the resistance to catastrophic crack propagation of ceramics under a critical temperature difference, ΔT_c.[23] R_{st} indicates the resistance to crack repropagation after a critical temperature difference, ΔT_c. From these three equations, high values of R^{IV} required TiC with a large E and v and low σ, whereas just the opposite is desired for TiC with high values of R. Therefore, these basic properties of TiC, such as σ, E, K_{IC}, α, and γ_f need to be considered synthetically in improving thermal shock resistance of TiC.

Table 2 gives the mechanical and thermophysical properties of monolithic TiC and the C_f/TiC composite. With carbon fiber addition, the strength, fracture toughness and thermal diffusivity of TiC are increased, and the elastic modulus and thermal expansion coefficient are decreased. The thermal shock parameters are also calculated and given in Table 3. The thermal stress fracture resistance parameter, R, the thermal stress damage parameter, R^{IV}, and thermal stress crack stability parameter, R_{st} of TiC are greatly increased with fiber addition. The increases of R, R^{IV} and R_{st} are 76, 81 and 138%, respectively. The results above further confirm that the addition of carbon fiber to TiC has beneficial effect on the thermal shock resistance of TiC.

Table 2
Properties of monolithic TiC and C_f/TiC composite

	TiC	C_f/TiC
Relative density, %	98.2	97.6
Elastic modulus, GPa	467±31	416± 38
Flexural strength, MPa	471±57	593±49
Fracture toughness, MPa $m^{1/2}$	4.06±0.53	6.87±0.72
Thermal expansion coefficient (20–1000°C), $\times 10^{-6}$ K^{-1}	7.73	6.22
Thermal diffusivity (400°C), $\times 10^{-6}$ m^2 s^{-1}	1.1	1.7

Table 3
Thermal shock resistance parameters of monolithic TiC and C_f/TiC composite and the residual strength rate when $\Delta T = 1400$°C

	TiC	C_f/TiC
$R=\sigma(1-v)/\alpha E$, K[a]	130(1-v)	229(1-v)
$R^{IV}=(K_{IC}/\sigma)^2/(1-v)$, μm[a]	74.3/(1-v)	134.2/(1-v)
$R_{st}=\gamma/\alpha^2 E$, $\mu m^{1/2}$ K[a]	789	1878
Residual strength rate ($\Delta T=1400$°C)σ_r/σ_0, %	32.5	42.5

[a] Flexual but not tensile strengths were used to calculate the R and R^{IV}. In the calculation of R_{st}, γ was converted according to the Irwin equation: $K_{IC}^2 = 2\gamma E$.

From Fig. 4 and Table 3, it can be seen that the σ_r-ΔT curves of monolithic TiC and the C_f/TiC composite have relatively good relationships with the calculated parameters R, R^{IV}, and R_{st}. The critical temperature difference, ΔT_c, for strength degradation increases with carbon fiber addition, which is consistent with the change of parameter R values shown in Table 3. However, the calculated R given in Table 3 are much lower than the experimental ΔT_c values shown in the curves in Fig. 4, this may be caused by the water-quenching speed. Insufficiently rapid quenching and the limit of water cooling rate could make the actual temperature difference the specimens experienced lower than the recorded temperature difference. Nevertheless, the factor does not influence the changing tendency of ΔT_c with the addition of carbon fibers. The decrement of strength decreases with carbon fiber addition for $\Delta T > \Delta T_c$ (Fig. 4), and such a tendency could be more clearly seen from residual strength rate values (for $\Delta T = 1400$°C) shown in Table 3. This is roughly consistent with the change of parameter R_{st} shown in Table 3.

3.4. Role of carbon fibers

The increases of the room and elevated temperature strengths and residual strength of TiC are undoubtedly the direct contribution of the high strength of carbon fiber to the composite. A rule-of-mixture formulation is used to evaluate the strengthening effect of carbon fibers on the strength of TiC. For a unidirectional fiber reinforced composite, the strength of the composite, σ_c, is given by

$$\sigma_c = \sigma_f V_f + \sigma_m(1 - V_f) \quad (4)$$

where σ_m and σ_f are the strengths of the matrix and the fiber, respectively, V_f is the fiber content. The short fiber orientation is random in TiC matrix. By assuming the fiber angle, θ, is uniformly distributed from 0 to $\pi/2$ (Fig. 6) in the plane perpendicular to the hot-pressing direction, the contribution, σ_p, from the fibers to the C_f/TiC composite strength is approximately obtained by

$$\sigma_p = V_f\left(\int_0^{\pi/2} \sigma_f \cos^2\theta \, d\theta\right) = 0.5\sigma_f V_f \quad (5)$$

Then the theoretical strength, σ_c^*, of the composite is given by

$$\sigma_c^* = \sigma_p + \sigma_m(1 - V_f) = 0.5\sigma_f V_f + \sigma_m(1 - V_f) \quad (6)$$

Considering the damage of the fiber during fabricating, σ_f is taken as 2500 MPa instead of 2700 MPa and σ_f is also assumed as a constant in the range from room

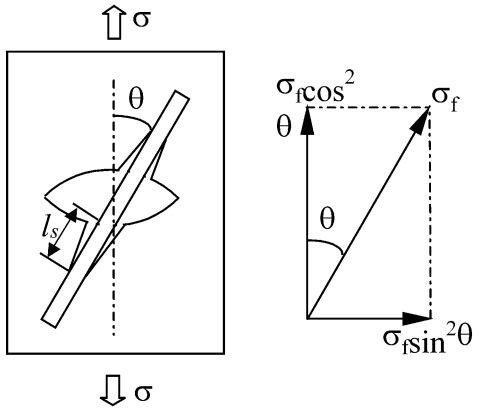

Fig. 6. An incline short fiber in the matrix.

temperature to 1400°C, V_f is 0.2. The tested strength value of monolithic TiC at various temperatures or under various thermal shock temperature differences are used as matrix strength value to calculate σ_c^*. Table 4 gives the calculated and experimental values of the strength of the composite at room temperature to 1400°C, experimental results are in good agreement with the calculated results, demonstrating the contribution of carbon fibers to the strength of the composite.

Table 5 gives the calculated and experimental values of the residual strength of the composite shocked at various thermal shock temperature differences. The calculated results of the residual strength basically agree with the experimental results when $\Delta T \leqslant 600$°C, and are lower than experimental results when ΔT exceeds 600°C and less than 1200°C, and are higher than the experimental results at $\Delta T \geqslant 1200$°C. This may be explained as follows. There is only a few of microcracks induced by thermal shock in the TiC matrix at $\Delta T \leqslant 600$°C (ΔT_c for monolithic TiC is 600°C), and the fibers are not damaged by thermal shock, thereby the calculated results of the residual strength agree with the experimental results. When ΔT exceeds ΔT_c (600°C) and less than 1200°C, the microcrack initiating and propagating in the C_f/TiC composite are prevented by carbon fibers compared with monolithic TiC, thus the matrix factual strength should be higher than the strength used in calculating, and consequently, the calculated results of the residual strength are less than the experimental results. When ΔT exceeds 1200°C, a great deal of microcracks are formed and then coalesce to form crack nets in the matrix, and the fibers and fiber/matrix interfaces may be also damaged because of the severe thermal shock, which decrease the strength of the composite. In contrast, the fiber strength is taken as a constant with ΔT in calculating. Therefore, the calculated results of residual strength of the composite are higher than the experimental results at $\Delta T \geqslant 1200$°C.

Fig. 7 shows stress–strain curves of the C_f/TiC composite unshocked and shocked at $\Delta T = 1200$°C, and these curves are nonlinear. The nonlinear behavior does not imply that the composite is plastic. In fact, this is a kind of pseudo-plasticity. The elastic modulus of the carbon fibers is less than that of TiC matrix (see Table 1), thereby the matrix carries more load than the fiber when it is deformed to the same strain. As the external load further increases, a lot of microcracks will be induced in the TiC matrix and the fiber with high rupture strength bridges the microcracks. Microcracks

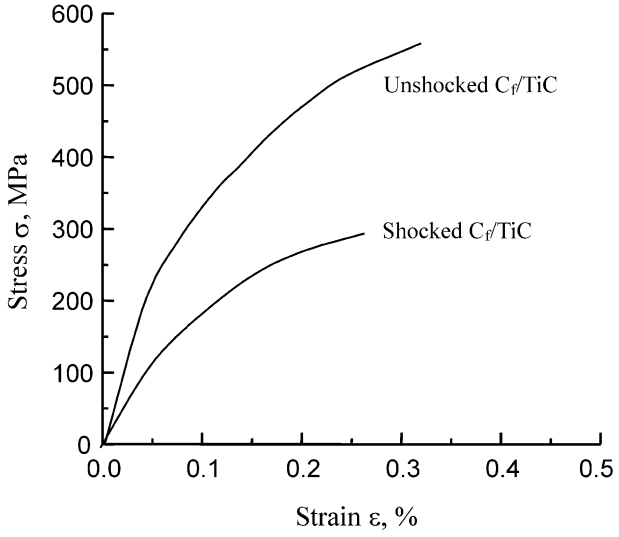

Fig. 7. Stress/strain curves of the C_f/TiC composites unshocked and thermal shocked, thermally shock temperature difference is 1200°C.

Table 4
Strength of the C_f/TiC composite at various temperatures

	20°C	1000°C	1200°C	1400°C
Measured strength, MPa	593	544	509	439
Calculated strength, MPa	627	549	503	448

Table 5
Residual strength of the C_f/TiC composite shocked at various thermal shock temperatures differences

	Thermal shock temperature difference, ΔT					
	0°C	600°C	700°C	900°C	1200°C	1400°C
Measured residual strength, MPa	593	602	584	533	278	252
Calculated residual strength, MPa	627	612	520	420	390	372

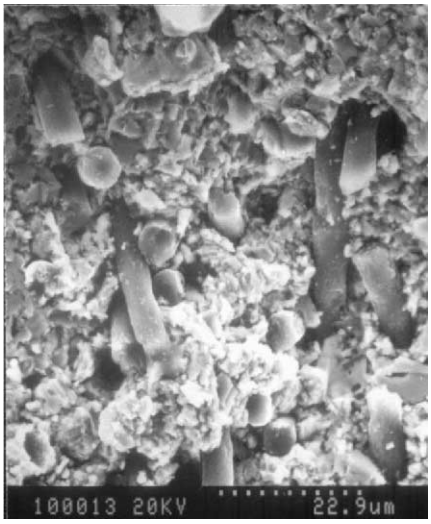

Fig. 8. Fracture surface of the C_f/TiC composite thermally shocked, thermal shock temperature difference is 1200°C.

initiating and propagating in the matrix cause a macro strain, as if there is a plastic deform in the composite. Because the fibers bridge the microcracks and prevent the cracks from propagating, the external load can be continuously increased. The nonlinear behavior indicates that the crack propagates in a quasi-static manner. This kind of pseudo-plasticity of ceramic composites has also been reported in many papers.[13, 24]

Fig. 8, a micrograph of the fracture surface of the C_f/TiC composite shocked at $\Delta T = 1200$°C, which shows fiber pullout, fiber bridging, and crack deflection. The existence of carbon fibers is very beneficial to mitigating instantaneous crack propagation. Based on the observed results from Figs. 3 and 8, fiber pullout, crack bridging and crack deflection should be the toughening mechanisms of the C_f/TiC composite.

The addition of carbon fibers to TiC increases the strength, σ, and the fracture toughness,K_{IC}, of TiC materials, and decreases the thermal expansion coefficient, α, and the elastic modulus,E. By changing the values of σ, K_{IC}, E and α, the thermal stress fracture parameter, R, the thermal stress damage resistance parameter, R^{IV}, and the thermal stress crack stability parameter, R_{st}, are all increased. In addition, the thermal diffusivity is also increased from 1.1×10^{-6} m^2 s^{-1} for monolithic TiC to 1.7×10^{-6} m^2 s^{-1} for C_f/TiC composite. From the point of view of decreasing the temperature gradient of the composite during thermal shocking, the increase of the thermal diffusivity is beneficial to improving the thermal shock resistance.

4. Conclusions

The addition of 20 vol.% short carbon fiber increases the room temperature flexural strength from 471 MPa for monolithic TiC to 593 MPa for the composite. The fracture strength of the composite at 1400°C is 439 MPa, an increase of 78% over that of monolithic TiC. A role-of-mixture formulation is proposed to calculate the strengthening effect of the carbon fibers, the calculated results of the strength of the composite in the range of room temperature to 1400°C agree well with the experimental results.

With carbon fiber addition, the fracture toughness of TiC is increased remarkably, and the elastic modulus and thermal expansion coefficient are decreased. The thermal stress fracture resistance parameter, R, thermal stress damage resistance parameter, R^{IV}, and thermal stress crack stability parameter, R_{st}, are all increased. The residual strength of the composite decreases significantly when the thermal shock temperature difference, ΔT, is higher than 900°C, and the residual strength is 252 MPa when ΔT is 1400°C. Carbon fiber reinforced-TiC composite exhibits superior resistance to thermal shock damage compared with monolithic TiC. Catastrophic failure induced by severe thermal stresses can be prevented in the C_f/TiC composite.

Acknowledgements

The authors would like to express their sincere thanks to Dr. Ying-Kui Guo and Dr. Guang-Wu Wen for the hot pressing of the materials. Financial support was partly provided by the China Postdoctoral Science Foundation.

References

1. Goetzel, C. G., *Cermets, ASM Handbook,* Vol. 7. American Society for Metals, Ohio, 1993 pp. 799–815.
2. Storms, E. K., *The Refractory Carbides*. Academic Press, New York, 1967 pp. 3–5.
3. Endo, H., Ueki, M. and Kubo, H., Microstructure and mechanical properties of hot-pressed SiC–TiC composites. *J. Mater. Sci.,* 1991, **26**, 3769–3774.
4. Endo, H., Ueki, M. and Kubo, H., Hot pressing of SiC-TiC composites. *J. Mater. Sci.,* 1990, **25**, 2503–2506.
5. Liu, N., Jiang, Y., Liu, Q. R., Xiong, W. H., Cui, K. and Hu, Z. H., Effect of chemical composition on the fracture toughness of Ti(C,N) based cermets. *Powd. Metall. Technol.,* 1999, **17**(4), 269–272 (in Chinese).
6. Han, I. S., Woo, S. K., Bai, K., Hong, K. S., Seo, D. W. and Chung, Y. J., Densification of reaction of bonded TiC composite by infiltration of liquid phase Ni/Si/Co. *J. Korean Ceram. Soc.,* 1998, **35**(10), 1020–1029.
7. Plucknett, K. P., Becher, P. F. and Subramanian, R., Melt-infiltration processing of TiC/Ni_3Al composites. *J. Mater. Res.,* 1997, **12**, 2515–2517.
8. Subramanian, R., Schneibel, J. H., Alexander, K. B. and Plucknett, K. P., Iron aluminide-titanium carbide composites by pressureless melt-infiltration-microstructure and mechanical properties. *Script. Mater.,* 1996, **35**, 583–588.
9. Schneibel, J. and Subramanian, H. R., The ductile-brittle size transition of iron aluminide ligaments in an FeAl/TiC composite. *Acta Mater.,* 1998, **46**, 4733–4741.

10. Durlu, N., Titanium carbide based composites for high temperature applications. *J. Eur. Ceram. Soc.,* 1999, **19**, 2415–2419.
11. Wang, H. R. and Singh, N., Thermal shock behavior of ceramics and ceramic composites. *Int. Mater. Rev.,* 1994, **39**, 228–244.
12. Jia, D. C., Zhou, Y. and Lei, T. C., Thermal shock resistance of SiC whisker reinforced Si_3N_4 ceramic composites. *Ceram. Inter,* 1996, **22**, 107–112.
13. Jia, D. C. *Microstructure and Thermal Shock Resistance of SiC Whisker Reinforced Si_3N_4, SiO_2 Ceramic Composites*. Ms thesis, Harbin Institute of Technology, Harbin, 1994, pp. 86–92.
14. Wen, G. W., *Study on Fused Quartz Glass Reinforced by Particles and Short Fibers*. PhD thesis, Harbin Institute of Technology, Harbin, 1996, pp. 89–120.
15. Kamiya, A., Nakano, K. and Kondoh, A., Fabrication and properties of hot-pressed SiC whisker-reinforced TiB_2 and TiC composites. *J. Mater. Sci. Lett.,* 1989, **8**(5), 566–568.
16. Birchall, J. D., Stanley, D. R., Mockford, M. J., Pigott, G. H. and Pinto, P. J., Toxicity of silicon carbide whiskers. *J. Mater. Sci. Lett.,* 1988, **7**, 350–352.
17. Zhou, X. G., Zhang, C. R., He, X. B., Li, Y. K., Zhou, A. B. and Cao, Y. B., A study on the hot press of pyrolysised carbon coated carbon fiber reinforced silicon carbide composite. *Mater. Eng.,* 2000, **3**, 39–41 (in Chinese).
18. Kosolapova, T. Y., *Handbook of High Temperature Compounds: Properties, Production, and Application*. Hemisphere Publication Corporation, New York, 1990.
19. Hu, B., *Preparation of Several Materials for Elevated Temperature Application*. Bachelor thesis, Harbin Institute of Technology, Harbin, 1996, pp. 19–32.
20. Chtterjee, D. K., Mendiratta, M. G. and Lipsitt, H. A., Deformation behaviour of single crystals of titanium carbide. *J. Mater. Sci.,* 1979, **14**, 2151–2156.
21. Das, G. K. S., Mazdiyasni, K. S. and Lipsitt, H. A., Mechanical properties of polycrystalline TiC. *J. Am. Ceram. Soc.,* 1982, **65**, 104–110.
22. Kingery, W. D., Factors affecting thermal stress resistance of ceramic materials. *J. Am. Ceram. Soc.,* 1955, **38**, 3–15.
23. Zhang, Q. C., *Mechanical Properties of Ceramic Materials*. Chinese Science Press, Beijing, 1987 pp. 279–304.
24. Borom, M. D. and Johnson, C. A., Thermomechanical mismatch in ceramic-fiber reinforced glass-ceramic composites. *J. Am. Ceram. Soc.,* 1987, **70**(1), 1–8.